Original Article

Three Medial All Suture Anchors Improves Contact Force Compared to Two Hard Body Anchors in a Biomechanical Two-Tendon Rotator Cuff Tear Model

Tammy R. Hoffman, Joseph D. Lamplot, M.D., Sarah J. McClish, Cassie Payne, and Patrick J. Denard, M.D.

Purpose: To biomechanically compare a knotless double-row construct with 3 medial all-suture (3AS) anchors with a standard 2 medial hard body (2HB) anchor construct. **Methods:** Twelve matched cadaveric shoulder specimens with a mean age of 57 years (range: 54-61 years) were randomized to receive a knotless double-row repair with either a 3AS or 2HB construct. In the 3AS construct, three 2.6-mm all-suture anchors were placed adjacent to the articular margin and secured laterally with two 4.75-mm knotless hard body anchors. In the 2HB construct, two 4.75-mm medial hard body anchors were placed medially, lateral fixation was identical to the 3AS construct. Creep, displacement, stiffness, and ultimate load were recorded for each sample. In addition, a SynDaver model was used to compare contact pressure between the 2 repair constructs. **Results:** There were no differences in cyclic displacement at 1, 30, and 100 cycles ($P = .616$, .497, .190, respectively), cyclic stiffness (.928), ultimate load (.445), or load to failure ($P = .445$) between the 2 constructs. The 3AS repair construct had improved contact pressure between tendon and bone when compared with the 2HB construct at loads of 20 N, 30 N, and 40 N ($P = .01$, .02, and .04, respectively). **Conclusions:** Displacement and load to failure properties are similar between knotless constructs using either 2HB or 3AS for the medial row. However, contact force may improve with the use of 3 medial all-suture anchors. **Clinical Relevance:** As all-suture anchors are smaller in size when compared with hard body anchors. For this reason, there is potential to place an additional all-suture medial anchor to improve contact force and potentially improve rotator cuff healing when compared with the use of hard body anchors.

A variety of techniques can be used to repair rotator cuff tears, including single-row repair, double-row (DR) repair, and transosseous-equivalent repair.[1] From a biomechanical standpoint, the goals of a rotator cuff repair are to maximize strength and increase contact force at time zero. Single-row repairs use a low-tension compression of the tendon to the tuberosity.[2] While this technique has been found to be effective for small tears, it is less likely to restore the anatomical footprint of the rotator cuff[3] and is associated with greater retear rates when compared with other construct types.[4-7] To address these shortcomings, particularly for larger rotator cuff tears, DR rotator cuff repairs were developed.[8-10] The initial suture-bridging DR repairs used constructs with two 5.5-mm medial hard body (HB) anchors linked to 2 lateral knotless anchors.[1] Unfortunately, failure of healing has continued to be observed, especially with increasing tear size, degree of fatty atrophy, and patient characteristics. One strategy to address this is placing additional anchors to increase the number of points of fixation.[11] However, these constructs are limited by suture anchor size and relative amount of available tuberosity footprint.

In recent years, all-suture (AS) anchors have been introduced as alternatives to HB anchors. Biomechanical investigations have demonstrated that these anchors have sufficient pull-out strength[12-14] and radiographic performance to be used as medial anchors for arthroscopic rotator cuff repair.[15] A distinct advantage of AS anchors is the approximately 50% reduction in size (e.g., 2.6-2.8 mm) compared with HB anchors (e.g., 4.5-5.5 mm), which allows less violation of the medial footprint. Given the smaller size, there is potential to increase the points of fixation and contact force of DR repairs.

The purpose of this study was to compare load to failure and displacement of knotless DR constructs performed with either 3 medial all-suture (3AS) anchors or 2 hard body (2HB) anchors in a human cadaveric large rotator cuff tear model. We hypothesized that there would be no difference in load-to-failure or cyclic displacement between the 2 constructs, but that contact force would be increased with the 3AS construct.

Methods

Test Groups

A biomechanical investigation was performed using 12 fresh-frozen matched pairs of male cadavers with a mean age of 57 years (range, 54-61 years). Due to the cadaveric nature of this study, institutional review board approval was not required.

Specimens were stored at −19°F and were thawed overnight at room temperature before repairs. Once thawed, the humerus was transected and potted in cylindrical fiberglass resin (Bondo; 3M, St. Paul, MN). The rotator cuff tendon was inspected to confirm the absence of any tearing or footprint disruption before the creation of the rotator cuff tear model. A complete tear of the supraspinatus and infraspinatus tendons was created. Beginning just posterior to the biceps tendon and advancing to the posterior margin of the infraspinatus tendon, the insertion the tendons were sharply elevated from the greater tuberosity with a no. 11 blade knife. The biceps tendon was left intact.

Repair Constructs

Each side of the matched cadaver pairs was randomized to a knotless DR rotator cuff repair with 1 of 2 techniques: 3 medial AS anchors (FiberTak Bridge; Arthrex, Naples, FL) or 2 medial HB anchors (Speed-Bridge; Arthrex) (Fig 1). Repairs were performed by 2 authors (P.J.D. and J.D.L.) who each performed half of the repairs. The repairs were performed in an open manner for testing purposes.

In the 3AS repair construct, three 2.6-mm anchors (FiberTak DR; Arthrex), each with 2 suture tape limbs were first placed in the greater tuberosity adjacent to the articular margin. The anterior anchor was placed 5 mm posterior to the biceps tendon. The posterior anchor was placed at the most posterior aspect of the original infraspinatus insertion. A third anchor was then placed halfway between the anterior and posterior anchors. The suture limbs from the anchors were then sequentially shuttled through the rotator cuff tendon, approximately 5 mm lateral to the musculotendinous junction. The 2 limbs from each anchor were shuttled together through the rotator cuff with an antegrade suture passer and a looped suture (FiberLink; Arthrex) in line with each anchor for a total of 3 equally spaced passes. One limb from each anchor was then selected and secured anterolaterally 10 mm distal to the lateral edge to edge of the greater tuberosity with a knotless anchor (4.75-mm SwiveLock; Arthrex) in line with the anterior medial row. This was repeated posteriorly, in line with the most posterior medial row anchor. Slack in the construct was removed manually prior to securing each lateral anchor.

In the 2HB construct, 2 medial anchors (4.75-mm SwiveLock; Arthrex) preloaded with FiberTape (Arthrex) were used. Anterior and posterior anchor placement was identical to the 3AS construct. A total of 2 suture passes (one for each anchor) was used to shuttle the FiberTape limbs through the rotator cuff in line with the anchors. Lateral fixation was performed identical to the 3AS construct.

Biomechanical Testing

Specimens were tested on a uniaxial Servo Hydraulic Instron Mechanical Testing System (Instron, Norwood, MA) with a 5 kN load cell (Fig 2). At the Instron's base, a variable angle platform with attached aluminum custom fixture was mounted and set to a 45 to 55° angle. Angle position was monitored through use of a calibrated Wixey digital angle gauge. A custom made
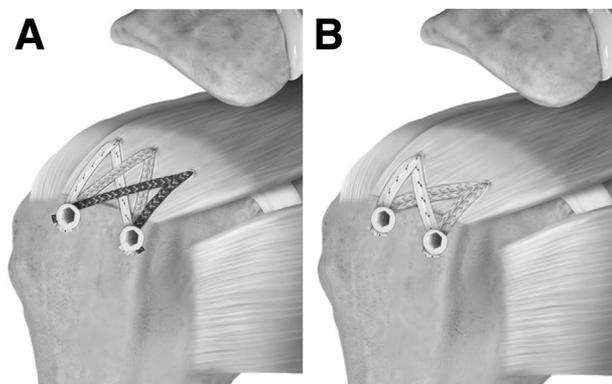
Fig 1. Schematics of the repair constructs in a right shoulder, which were evaluated biomechanically. (A) Repair using 3 medial all-suture anchors and 2 lateral hard body anchors. (B) Repair using 2 medial hard body with 2-mm tape and 2 lateral hard body anchors.
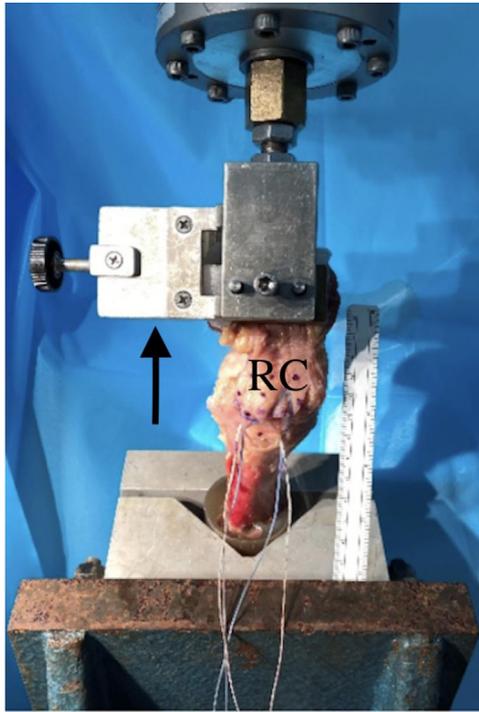
Fig 2. Photograph of the testing assembly, which consists of a uniaxial Servo Hydraulic Instron Mechanical Testing System, a variable angle platform, and attached aluminum custom fixture. Arrow indicates the line of pull during testing. (RC, the rotator cuff.)

cryo clamp was attached to the actuator and load cell was calibrated using WaveMatrix software (Instron). The humeral potting was clamped within the aluminum fixture, and adjustments to the variable angle platform position were made to ensure that the supraspinatus tendon was directly in line with that of the actuator's long axis. To ensure reliable fixation within the cryo clamp, the actuator was lowered to the specimen as much as possible in efforts to not clamp solely to muscle tissue (gauge length ∼25 mm). With a tissue marker, several points were drawn on the supraspinatus tissue medial to the anchors placed adjacent to the articular margin (between the repair and the cryo clamp interface). A surgical ruler was attached to the test fixture within the field of view of the repair site to assist in calibrated measurements later for creep analysis. Once tissue was frozen within the clamp, a tensile load of 10 N was applied for a 2-minute duration. Cycling in load control was followed between 10 and 160 N for 100 cycles at a frequency of 1 Hz. Postcycling, specimens were pulled to failure at a loading rate of 1 mm/sec until catastrophic failure.

Biomechanical Data

Creep (stretch of tissue under constant load profile) was calculated with ImageJ software (National Institutes of Health, Bethesda, MD) by tracking translation of key points on the supraspinatus during the 10-N hold phase of the testing sequence. More specifically, to determine total tissue creep, photos of the specimen were taken at the start of the 2-minute hold, and at its conclusion. With the surgical ruler in view, the software was calibrated to recognize the number of pixels that equates to a distance (in millimeters), resulting in our creep outcome. The remaining outcomes were calculated by analyzing the plotted load-displacement curve of each sample. Within the cycling phase of testing, cyclic displacement and cyclic stiffness values were calculated at multiple points (cycle 1, 30, and 100) to track biomechanical responses to loading. Cyclic displacement corresponded to actuator displacement from the genesis of the cycling phase to the last point of the cycle being analyzed. Intracyclic stiffness was defined as the slope of the curve between 55 and 155 N of the given cycle. Stiffness (slope of the load-displacement curve) directly following the cycling phase was also calculated, as well as total displacement at 200 N, and ultimate load. Ultimate load was defined as the maximum load recorded up to catastrophic failure.

Footprint Testing

To compare the footprint compression of both constructs, TekScan pressure measurements were performed with a Model #4205-12 Matrix Sensor. The TekScan system allows for detailed pressure mapping of the constructs (Fig 3). Sensitivity was adjusted so that the maximum expected load of about 55 N would not be oversaturated. The sensors were calibrated using a 2-point calibration at 5 and 55 N. To limit variability, SynDaver rotator cuff tendon models were used for testing (Fig 2). This patented synthetic material was designed and validated to mimic the tensile modulus, abrasion resistance, coefficient of friction, and other imperative mechanical properties of rotator cuff tendon that is intended to simulate. While the SynDaver method excludes the use of the cadaveric tendon, it allows consistent and comparable results of the constructs that were investigated. This technique was used on each repair construct under loads of 0, 10, 20, 30, and 40 N.

Statistical Analysis

The primary outcome of interest was that of contact force (N) between tendon to bone. A prior power analysis was performed based on results from Kaplan et al.[16] Using an alpha level of 0.05 and a desired power of 0.80, it was determined that a total of 6 samples in each group were required to detect a 238N difference in load to failure between the 2 groups. One-way repeated measures analysis of variance and *t* tests were used to statistically compare the supraspinatus contact force of the 2HB and 3AS groups. In addition, linear regression analyses were performed on the contact force for each repair construct.
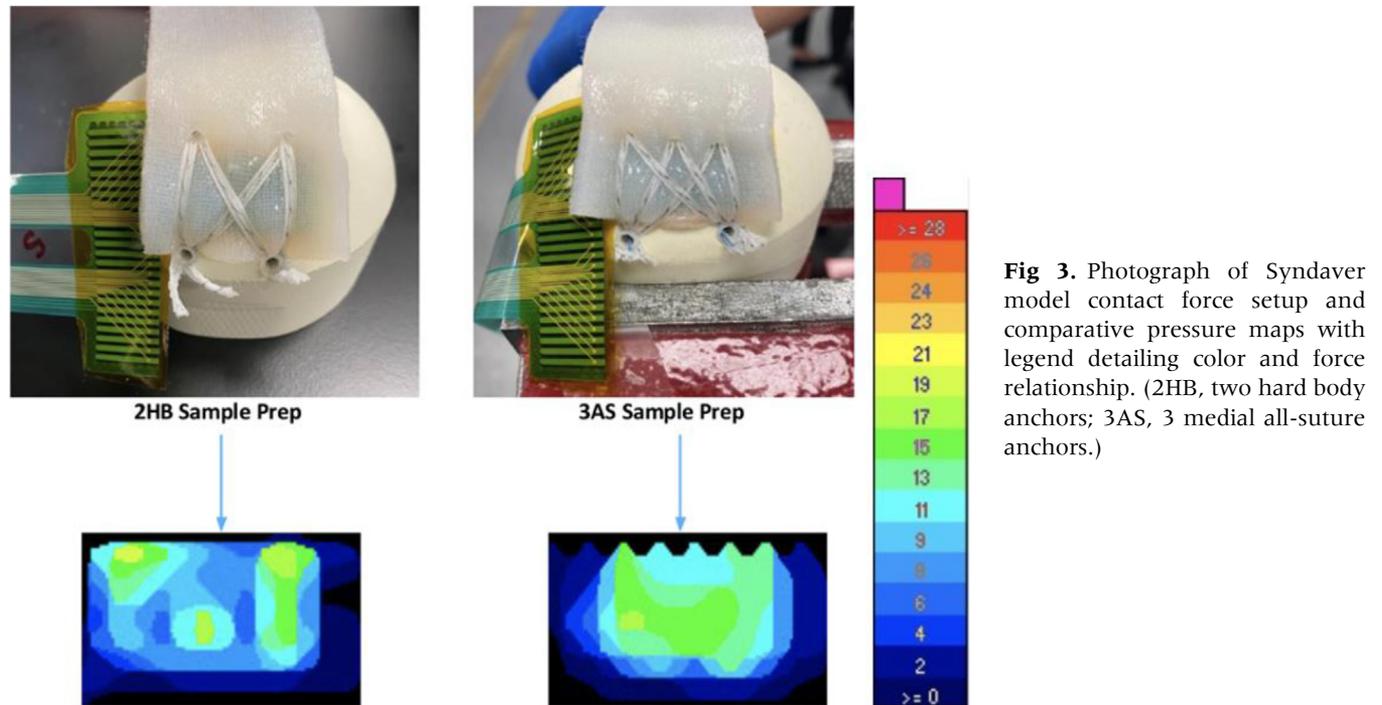
Fig 3. Photograph of Syndaver model contact force setup and comparative pressure maps with legend detailing color and force relationship. (2HB, two hard body anchors; 3AS, 3 medial all-suture anchors.)

Results

Biomechanical testing data are summarized in Table 1. There were no differences between constructs with regards to cyclic displacement at 1, 30, and 100 cycles ($P = .616$, 0.497, 0.190, respectively) or cyclic stiffness ($P = .928$, Fig 4).

There was no difference in load to failure ($P = .445$). In the 3AS construct, the mode of failure was lateral anchor pull-out in 3 cases, medial tendon tearing in 2 cases, and medial anchor pull-out in 1 case. In the 2HB group, the mode of failure was lateral anchor pull-out in 4 cases and medial tendon tearing in 2 cases.

Table 1. Biomechanical Comparison of the 3AS and 2HB Constructs

Outcome Data	3AS	2HB	P Value
Creep, mm	0.35 ± 0.2	0.21 ± 0.1	.275
Cyclic displacement, mm			
1 cycle	1.41 ± 1.0	1.57 ± 1.0	.616
30 cycles	1.95 ± 0.8	1.73 ± 0.6	.497
100 cycles	3.64 ± 2.5	2.78 ± 1.5	.190
Cyclic stiffness, N/mm			
Cycle 1	58.4 ± 46.4	56.1 ± 36.0	.928
Cycle 30	78.4 ± 30.1	74.8 ± 23.6	.822
Cycle 100	80.9 ± 30.9	77.0 ± 23.1	.810
Postcyclic stiffness, N/mm	76.8 ± 13.2	81.53 ± 23.7	.649
Displacement at 200 N, mm	7.62 ± 2.3	8.10 ± 3.9	.749
Load to failure, N	718.2 ± 344.0	608.7 ± 134.5	.445

2HB, two hard body anchors; 3AS, 3 medial all-suture anchors.

Footprint Contact

Contact force increased linearly with progressive load for both constructs. There was no significant difference between constructs at 0 N or 10 N ($P = .06$ for both forces). In the 3AS contact force was improved by 25% at 20 N, 26% at 30 N, and 30% at 40 N compared with the 2HB construct. ($P = .01$, $P = .02$, and $P = .04$, respectively, Fig 5).

Discussion

The major findings of this study were that there were no differences in cyclic displacement or load to failure between 2 knotless constructs with the traditional 2 medial HB anchors or 3 medial AS anchors in a 2-tendon tear rotator cuff model. However, there was improved contact force (N) with the use of the 3 medial anchor construct. These findings may have clinical implications for rotator cuff repair procedures.

Traditionally, knotless DR repairs were described with 2 medial and 2 lateral anchors, each 4.5 to 5.5 mm in size. More recently, AS anchors have increased in popularity due to their high pull-out strength despite their small size.12-14 Advantages of these anchors include ease of revision, decreased violation of the footprint, and improved postoperative imaging.[15,17] Studies have supported that repair of large rotator cuff tears are associated with decreased healing rates.[18,19] In one study, the risk of retear was increased 2.29 times with every 1 cm of increased tear size.[20]
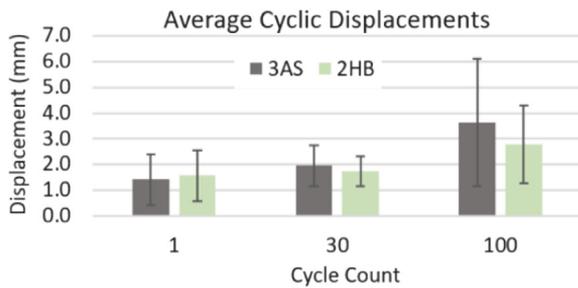
Fig 4. Average cyclic displacements by 1, 30, and 100 cycle counts of 3AS and 2HB techniques. (2HB, two hard body anchors; 3AS, 3 medial all-suture anchors.)

While variability in tissue quality exists, one strategy to mitigate failure risk is to increase the number of points of fixation with 3 medial anchors, given that the weak link in rotator cuff repair is the suture−tendon interface.[21] However, there is a trade-off between footprint violation (which the rotator cuff must heal to) and number of points of fixation, particularly with traditionally sized HB anchors. With AS anchors, in contrast, increased points of fixation can be achieved despite the placement of additional anchors, with some AS anchors violating an even smaller amount of footprint. In the current model, for example, placement of three 2.6-mm medial anchors equated to an 18% reduction in footprint violation compared to the use of two 4.75-mm anchors.

As we hypothesized, there was no difference in load to failure or cyclic displacement between the constructs in the current study. The load to failure of the 2HB and 3AS constructs (609 and 718 N, respectively) was consistent with previously reported biomechanical evaluations of DR repairs. In a matched pair analysis of DR constructs with #2 polyblend suture and medial knots with HB anchors, Park et al.[22] reported a load to failure of approximately 600 N. Regarding DR constructs with medial AS anchors, Bernardoni et al.[23] compared 2 AS anchors or 2 HB anchors in DR constructs with medial knots. Load to failure was 618 N in the all-suture anchor group and 545 N in the hard body anchor group ($P = .34$). In concert with our findings, this provides evidence that the use of smaller AS anchors medially, placed with or without knots, does not compromise the biomechanics of DR repairs.

Several factors contribute to rotator cuff healing, including fatty infiltration, tear size, and a variety of biologic factors. Biomechanical approaches to maximize healing include optimizing load to failure and contact area and minimizing displacement. Contact area in particular is felt to be important for achieving tendon healing.[24-26] While DR repairs have decreased the incidence of retear, overall retears rates remain at approximately 25%, and are notably increased with

larger tears.[27] Thus, it appears worthwhile to continue to attempt to maximize contact force in large and massive rotator cuff tears, given its direct relationship with area. Burkhart et al.[28] demonstrated that a construct with 2 medial and 3 lateral HB anchors increased contact area compared with a standard DR construct.[11] Previous authors have also described the use of 3 medial anchors for large and massive tears.[29,30] However, as mentioned previously, these approaches may be limited by available footprint per anchor size. Goschka et al.[31] compared the traditional hard body anchors with all-suture anchors determined that the latter reduces the occurrence of loose body complications as it requires a decreased amount of bone removal. Additionally, Ntalos et al.[32] determined that all-sure anchors are correlated to decreased bone damage in the case of pullout. In the current study using a massive rotator cuff tear model, contact force (N) was increased by up to 30% with the use of 3 medial anchors. This 30% increase in force was proportional to a 55% increase in surface area (m^2) in the 3AS construct. While further study is required, this ability to increase contact force with an overall decreased violation of the footprint may have clinical implications for large and massive rotator cuff tears.

A final consideration of the constructs evaluated in the current study is strain on the rotator cuff. DR repair techniques have been associated with more detrimental retear patterns as they introduce greater tendon strain at the musculotendinous junction[30] and are at risk for medial tissue failure.[33] Although not proven, this risk may potentially be decreased with tape-like sutures as used in the current study. Dias et al.[34] demonstrated that tape-like sutures decrease peak contact force compared to #2 sutures. Moreover, additional medial passes improved contact force as we observed with the 3AS, which had 3 medial passes compared with the
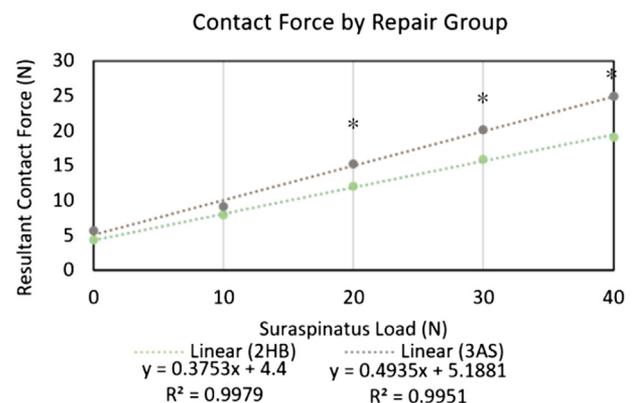
Fig 5. Contact force in Newtons (N) for the 2 hard body (2HB) and 3 medial all-suture (3AS) anchor constructs. Statistically significant differences were observed at 20, 30, and 40 N of load. Asterisks denote significance.

2 medial suture passes in the 2HB construct. Further investigation could examine medial strain between the constructs.

Limitations

There are several limitations to our study. The major limitation is the inability to reliably use a cadaveric model in contact force mapping as this introduces moisture into the sensor, skewing results. The results are limited to the rotator cuff tear model evaluated (2 tendon tear) and may not necessarily be extrapolated to small tears or tears involving the subscapularis tendon. The findings are limited to the biomechanical analysis and do not reflect biologic healing. The TekScan, for instance, has inherent limitations and it is possible that pressure could change under cyclic loading.

Conclusions

Displacement and load to failure properties are similar between knotless constructs using either 2 hard body or 3 all-suture anchors for the medial row. However, contact force may improve with the use of 3 medial all-suture anchors.

Acknowledgments

References

1. Dey Hazra RO, Ernat JJ, Rakowski DR, Boykin RE, Millett PJ. The evolution of arthroscopic rotator cuff repair. *Orthop J Sports Med* 2021;9:23259671211050899.
2. Hantes ME, Chalatsis GI, Mpakagiannis G. Single-row versus double-row repair in rotator cuff tears. In: Sozen S, ed. *Surgical recovery*. London: IntechOpen, 2019. https://www.intechopen.com/chapters/69582. Accessed July 23, 2022.
3. Karakus O, Karaman O, Sari AS, Saygi B. Difference in the results of repair made with single or double rows according to the shape and size of the tear in arthroscopic rotator cuff surgery. *Medicine (Baltimore)* 2021;100(32).
4. Longo UG, Carnevale A, Piergentili I, et al. Retear rates after rotator cuff surgery: A systematic review and meta-analysis. *BMC Musculoskelet Disord* 2021;22:749.
5. Lapner P, Li A, Pollock JW, et al. A multicenter randomized controlled trial comparing single-row with double-row fixation in arthroscopic rotator cuff repair: Long-term follow-up. *Am J Sports Med* 2021;49:3021-3029.
6. Kataoka T, Mifune Y, Inui A, et al. Combined therapy of platelet-rich plasma and basic fibroblast growth factor using gelatin-hydrogel sheet for rotator cuff healing in rat models. *J Orthop Surg Res* 2021;16:605.
7. Pandey V, C J Mfume, Mathai NJ, Madi S, Karegowda LH, Willems J. Five year follow up of retrospective cohort comparing structural and functional outcome of arthroscopic single-row versus double-row suture bridge repair of large posterosuperior rotator cuff tear in patients less than or equal to 70 years. *Arch Bone Joint Surg* 2021;9: 391-398.
8. Lo IK, Burkhart SS. Double-row arthroscopic rotator cuff repair: Re-establishing the footprint of the rotator cuff. *Arthroscopy* 2003;19:1035-1042.
9. Park MC, ElAttrache NS, Tibone JE, Ahmad CS, Jun BJ, Lee TQ. Part I: Footprint contact characteristics for a transosseous-equivalent rotator cuff repair technique compared with a double-row repair technique. *J Shoulder Elbow Surg* 2007;16:461-468.
10. Sano H, Komatsuda T, Inawashiro T, et al. Comparison between single and double suture passing techniques in the suture bridge rotator cuff repair with a 2-mm tape: A simulation study using a three-dimensional finite element method. *J Orthop Sci* 2021;26:207-212.
11. Endo A, Hoogervorst P, Safranek C, et al. Linked double-row equivalent arthroscopic rotator cuff repair leads to significantly improved patient outcomes. *Orthop J Sports Med* 2020;8:2325967120938311.
12. Barber FA, Herbert MA. All-suture anchors: Biomechanical analysis of pullout strength, displacement, and failure mode. *Arthroscopy* 2017;33:1113-1121.
13. Godry H, Jettkant B, Seybold D, Venjakob AJ, Bockmann B. Pullout strength and failure mode of industrially manufactured and self-made all-suture anchors: A biomechanical analysis. *J Shoulder Elbow Surg* 2020;29:1479-1483.
14. Ergün S, Akgün U, Barber FA, Karahan M. The clinical and biomechanical performance of all-suture anchors: A systematic review. *Arthrosc Sports Med Rehabil* 2020;2: e263-e275.
15. Memon KA, Dimock R, Bernasconi A, et al. Clinical and radiological outcomes of rotator cuff repairs using all-suture anchors as medial row anchors. *Arch Bone Joint Surg* 2019;9:527-535.
16. Kaplan K, ElAttrache NS, Vazquez O, Chen YJ, Lee T. Knotless rotator cuff repair in an external rotation model: The importance of medial-row horizontal mattress sutures. *Arthroscopy* 2011;27:471-478.
17. Cho CH, Bae KC, Kim DH. Biomaterials used for suture anchors in orthopedic surgery. *Clin Orthop Surg* 2021;13: 287-292.
18. Morihara T, Kida Y, Furukawa R, et al. Therapeutic outcomes of muscular advancement by an arthroscopic-assisted modified Debeyre-Patte procedure for irreparable large and massive rotator cuff tears. *J Orthop Sci* 2018;23: 495-503.
19. Iijima Y, Matsuki K, Hoshika S, et al. Relationship between postoperative retear and preoperative fatty degeneration in large and massive rotator cuff tears: Quantitative analysis using T2 mapping. *J Shoulder Elbow Surg* 2019;28:1562-1567.
20. Nho SJ, Brown BS, Lyman S, et al. Prospective analysis of arthroscopic rotator cuff repair: Prognostic factors affecting clinical and ultrasound outcome. *J Shoulder Elbow Surg* 2009;18:13-20.
21. Wang Z, Long Z, Li H, et al. A biomechanical comparison of a mesh suture to a polyblend suture in a porcine tendon model. *Ann Transl Med* 2021;9:450.

22. Park MC, Peterson A, Patton J, McGarry MH, Park CJ, Lee TQ. Biomechanical effects of a 2 suture-pass medial inter-implant mattress on transosseous-equivalent rotator cuff repair and considerations for a "technical efficiency ratio." *J Shoulder Elbow Surg* 2014;23:361-368.

23. Bernardoni ED, Frank RM, Veera SS, et al. Biomechanical analysis of medial-row all-suture suture anchor fixation for rotator cuff repair in a pair-matched cadaveric model. *Arthroscopy* 2019;35:1370-1376.

24. Lima EBS, Godoy GP, Osés GL, et al. A simple technique to restore tension of a loose suture bridge during rotator cuff repair: Save the repair. *Arthrosc Tech* 2022;11: e409-e411.

25. Tanpowpong T, Itthipanichpong T, Limskul D. How to maximize suture tension in double-row suture-bridge rotator cuff repair? *Arthrosc Tech* 2021;10:e2207-e2212.

26. Mao Z, Fan B, Wang X, et al. A systematic review of tissue engineering scaffold in tendon bone healing in vivo. *Front Bioeng Biotechnol* 2021;9:621483.

27. Buyukdogan K, Aslan L, Koyuncu Ö, et al. Long-term outcomes after arthroscopic transosseous-equivalent repair: Clinical and magnetic resonance imaging results of rotator cuff tears at a minimum follow-up of 10 years. *J Shoulder Elbow Surg* 2021;30:2767-2777.

28. Burkhart SS, Denard PJ, Obopilwe E, Mazzocca AD. Optimizing pressurized contact care in a rotator cuff repair: the diamondback repair. *Arthroscopy* 2012;28: 188-195.

29. Lee BD, Gilmer BB, Lang SD, Guttmann D. A modified SpeedBridge technique for retracted or delaminated rotator cuff repairs. *Arthrosc Tech* 2019;25(8): e1373-e1378.

30. Hackl M, Nacov J, Kammerlohr S, et al. Intratendinous strain variations of the supraspinatus tendon depending on repair technique: A biomechanical analysis regarding the cause of medial cuff failure. *Am J Sports Med* 2021;49: 1847-1853.

31. Goschka AM, Hafer JS, Reynolds KA, et al. Biomechanical comparison of traditional anchors to all-suture anchors in a double-row rotator cuff repair cadaver model. *Clin Biomech (Bristol, Avon)* 2015;30:808-813.

32. Ntalos D, Huber G, Sellenschloh K, et al. All-suture anchor pullout results in decreased bone damage and depends on cortical thickness. *Knee Surg Sports Traumatol Arthrosc* 2021;29:2212-2219.

33. Bedeir Y, Jimenez AE, Grawe BM. Recurrent tears of the rotator cuff: Effect of repair technique and management options. *Orthop Rev* 2018;10:7593.

34. Dias CE, Gonçalves SB, Completo A, et al. Why are tapes better than wires in knotless rotator cuff repairs? An evaluation of force, pressure and contact area in a tendon bone unit mechanical model. *J Exp Orthop* 2021;3(8):9.